Molecular Docking Simulations for Macromolecularly Imprinted Polymers

ARTICLE *in* INDUSTRIAL & ENGINEERING CHEMISTRY RESEARCH · OCTOBER 2011

Impact Factor: 2.59 · DOI: 10.1021/ie201858n · Source: PubMed

4 AUTHORS, INCLUDING:

Pengyu Ren
University of Texas at Austin
89 PUBLICATIONS **3,855** CITATIONS

SEE PROFILE

Published in final edited form as:
Ind Eng Chem Res. 2011 October 31; 50(24): 13877–13884. doi:10.1021/ie201858n.

Molecular docking simulations for macromolecularly imprinted polymers

David R. Kryscio[a], **Yue Shi**[b], **Pengyu Ren**[b], and **Nicholas A. Peppas**[a,b,*]

[a]The University of Texas at Austin, Cockrell School of Engineering, Department of Chemical Engineering, Austin, TX 78712, USA

[b]The University of Texas at Austin, Cockrell School of Engineering, Department of Biomedical Engineering, Austin, TX 78712, USA

Abstract

Molecularly imprinted polymers are fully synthetic antibody mimics prepared via the crosslinking of organic monomers in the presence of an analyte. This general procedure is now well developed for small molecule templates; however, attempts to extend the same techniques to the macromolecular regime have achieved limited success to date. We employ molecular docking simulations to investigate the interactions between albumin, a common protein template, and frequently employed ligands used in the literature at the molecular level. Specifically, we determine the most favorable binding sites for these ligands on albumin and determine the types of non-covalent interactions taking place based on the amino acids present nearby this binding pocket. Our results show that hydrogen bonding, electrostatic interactions, and hydrophobic interactions occur between amino acids side chains and ligands. Several interactions are also taking place with the polypeptide backbone, potentially disrupting the protein's secondary structure. We show that several of the ligands preferentially bind to the same sites on the protein, which indicates that if multiple monomers are used during synthesis then competition for the same amino acids could lead to non-specific recognition. Both of these results provide rational explanations for the lack of success to date in the field.

Keywords

molecularly imprinted polymers; macromolecular imprinting; molecular docking; protein conformation; albumin

1. Introduction

1.1. Molecularly imprinted polymers (MIPs)

Molecular recognition or molecular imprinting is an emerging field of interest in which a polymer network is synthesized in the presence of a template molecule. After polymerization, the template is removed which results in stereo-specific binding sites for this analyte of interest. Macromolecularly imprinted polymers – polymer networks synthesized in the presence of a macromolecular template – are of particular importance because they open up the field for a whole new set of applications that will lead to robust biomedical products, including as biosensors and undesirable analyte removers. Protein recognitive polymers are ideal replacements to their biological counterparts, antibodies,

*Corresponding author: peppas@che.utexas.edu (N.A. Peppas) The University of Texas at Austin, Department of Chemical Engineering, 1 University Station C0400, Austin, TX 78712-1062, Telephone: +1 512 471 6644, Fax: +1 512 471 8227.

because they can be tailored to a variety of templates, are inexpensive and straightforward to prepare, have greater stability in harsh conditions, and are reusable. In spite of the successes of molecularly imprinted polymers (MIPs) used for recognition of small molecular weight molecules, macromolecular recognitive MIPs have yet to reach their vast potential. This is due to the inherent properties of proteins which include conformational instability, large size, and complexity.

In general, MIPs are prepared via a simple process. First, components are selected based on the application of interest. Functional monomer(s) are chosen which exhibit chemical functionality designed to interact with the template molecule (analyte of interest) via covalent or non-covalent chemistry. Also, the type and amount of cross-linking monomer is selected which will provide structural support to the polymer network as well as define the pore size for diffusion of the biomolecule into and out of the matrix. Once chosen, these ingredients are dissolved, with the template, in an appropriate solvent. Second, the pre-polymerization complex is formed between the biomolecule and functional monomer(s) which forms the basis of the specific binding sites. The monomer mixture is then polymerized typically via free radical polymerization and lastly, the template is removed which leaves a polymer network with three-dimensional binding cavities based on the biomolecule of interest. For a more in depth overview of the field of molecular imprinting in both small molecular weight and macromolecular template areas, the reader should refer to several excellent previously published review articles.[1–6]

1.2. Macromolecularly imprinted polymers with computational modeling

Computational modeling techniques can provide examination of various constituents in the pre-polymerization solution in a much more efficient and cost effective manner. Molecular simulations have been employed successfully for rational design of small molecular weight MIPs.[7–12] To date, however, very few protein MIP computational studies have been reported.[13–16] Hsu et al.[13] employed molecular mechanics simulations to show changes in the secondary structure of ribonuclease A as a function of monomer (styrene) or crosslinker (polyethylene glycol 400 dimethacrylate) concentration. Pan et al.[16] used molecular docking between the template protein (*Staphylococcus aureus* protein A) and monomer (acrylamide) to conclude that H-bonding and hydrophobic interactions are the dominant driving forces for interactions in this pre-polymerization solution.

Levi and Srebnik[14] used lattice Monte Carlo simulations to investigate the effects of initiator, crosslinking agent, and monomer concentrations on the resultant protein imprinted polymer structure and functionality. They found that the presence of the protein template had no effect on the average structure of the resultant polymer and that highly charged pre-polymerization solutions led to non-specific interactions. These conclusions agree with previous independent experimental studies from Bergmann and Peppas [17] and Janiak et al.[18] In their most recent work, Levi and Srebnik[15] employed the same model to determine that monomer concentration in the pre-polymerization solution had the strongest influence on imprinting efficiency.

Although these results are interesting, the models neglect to address two of the key challenges facing successful protein recognition with MIPs – increased complexity and conformational stability of proteins relative to small molecular weight templates. It is clear that the success of a subsequent MIP is strongly dependent on the stability and strength of its monomer-template complex prior to polymerization. Despite the increased interest in this area over the past several years, few studies have seriously investigated the fundamental mechanisms behind template recognition, thus they largely remain unknown. It is widely accepted that non-covalent interactions, such as hydrogen bonding, electrostatic interactions, and hydrophobic interactions all play a role, but, the way in which these forces co-operate is

still in question. Our goal in this work was to use molecular docking to further investigate the types of interactions occurring between monomers and crosslinkers with protein templates prior to polymerization.

1.3. Overview of molecular docking

When the structure of a macromolecular target is known, typically from X-ray or NMR, molecular docking is commonly used as an enrichment tool for rapid virtual screening of large libraries of potential ligands. This technique is often used in lieu of high-throughput screening due to cost considerations with comparable, if not better, hit-rate enrichment.[19,20] In general, ligands are 'docked' into binding sites of a target (macromolecule) and possible poses of the small molecule are sampled according to a specific search algorithm. For each pose, a 'score' value is calculated via a scoring function, which is derived anywhere from molecular mechanics force fields such as AMBER,[21] OPLS,[22] and CHARMM,[23] to empirical free energy binding complexes.[24]

There are various approaches to molecular docking each with different search algorithms and scoring functions. Common packages include DOCK[25], GOLD[26], FlexX[27], and Glide[28] with selection dependent on the desired application and protein target. Overall, molecular docking provides reliable predictions of binding poses, but not binding affinity.[29,30] In fact, an evaluation of numerous docking programs found that the binding geometry was successful in predicting binding sites within 2 Å RMSD of experimental structures; however, the predicted binding affinity was weakly correlated with experimental data ($R<0.6$). [31]

While robust techniques like molecular mechanics based free energy simulation methods are becoming more accessible due to advances in high performance computing, docking studies remain an integral part of virtual screening. This is because molecular mechanics simulations are far more resource consuming relative to docking (on the order of days per target versus minutes).[29] The limitations of docking, however, lie in the lack of configurational sampling or protein targets and the crude description of solvent and electrostatic interactions for the sake of computational speed.[32] As a result, molecular mechanics or molecular dynamics methods, which affords considerably more accurate predictions of binding affinity,[33] is typically used only after docking has identified promising ligands.

1.4. Protein stability

Proteins fold spontaneously into their native three-dimensional conformations based solely on their sequence of amino acids.[34] Protein stability is a balancing act between large, opposing enthalpic and entropic contributions, which are dominated by hydrogen bonding, hydrophobic interactions, and configurational entropy. [35] The exact contributions of each of these influences to the stability of proteins remain in question. And because the native state of proteins are typically just 5–15 kcal/mol more stable than that of the unfolded,[36] they are highly sensitive to relatively small environmental changes, including temperature, pH, or salt/ligand concentration. For instance, the energy contribution of a single hydrogen bond in macromolecules is on the order of 2–5 kcal/mol.[36] However, many proteins will spontaneously refold into their native conformation once returned to the original environment.

Protein denaturation or unfolding involves the loss of secondary or tertiary structure, or both. Urea and guanidine hydrochloride are the two most commonly employed and studied protein denaturants; however, the exact mechanism of the denaturation remains intensely debated.[37] Indeed, Lim et al.[38] concluded that urea destabilizes proteins by disrupting

hydrogen bonds while Cauchi et al.[39] found that electrostatic and van der Waals forces dominate denaturation with H-bonding playing a minimal role. What does seem to be agreed upon is that chaotropic agents bind to the protein which reduces its chemical potential. Once the chemical potential falls below that of the native state, the protein unfolds.[37]

1.5. Impetus of molecular docking studies

In a previous report from our lab,[40] circular dichroism was used to clearly show the negative effect monomers and crosslinkers frequently employed in protein MIPs have on the native secondary structure of bovine serum albumin (BSA). The negative influence was seen for the five most commonly used monomers – acrylamide (Aam), methacrylic acid (MAA), aminophenylboronic acid (APBA), acrylic acid (AA), and N-isopropylacrylamide (NIPAam) – at concentrations far below what are used in the field. The degree to which BSA's structure was altered upon addition of relatively low amounts of these monomers is certainly a cause for concern and is potentially a large reason for the lack of success in the field to date. If the protein template is forced into a different conformation prior to polymerization, the binding sites formed during polymerization would be specific to this alternate state. When the polymer is re-exposed to the protein in its native state, specific recognition would not be observed.

Additionally, the two most frequently employed crosslinkers – N,N' methylenebisacrylamide (MBA) and ethyleneglycol dimethacrylate (EGDMA) – were investigated with BSA in an analogous manner. A similar result was obtained for MBA in that a substantial change in the native spectra of BSA was observed upon increasing amounts of MBA. However, the spectrum for BSA in the presence of EGDMA maintained its native characteristic shape. Even when the concentration of EGDMA was increased well above what is found in the literature, the decrease in helical structure was far less than what was seen for the other six ligands.

In this work, molecular docking was used to further investigate the results from these circular dichroism studies. Namely, docking studies with the same seven ligands – Aam, MAA, APBA, AA, NiPAam, MBA, and EGDMA – were performed on human serum albumin (HSA) to determine the most favorable binding site. Based on the top ranked poses, we determined the amino acids which the monomers preferentially bind as well as the types of interactions taking place. The distance between the amino acid and the ligand as well as the side group present on the residue provides an indication of the type of interaction occurring. A general rule of thumb is that interactions are taking place if heavy atoms of the ligand and amino acid are within approximately 4.0 Å of each other. For example, distances of 2.6–3.4 Å between the appropriate atoms (hydrogen donor and acceptor of electronegative atom) is indicative of hydrogen bonding.[26,41] Ultimately, the functional groups involved dictate the type of non-covalent interaction occurring – hydrogen, electrostatic or hydrophobic – as long as the two atoms are roughly within 4 Å of each other. This analysis allowed for a more robust explanation of the mechanism behind the change in conformation. Also, we were able to hypothesize which interactions were most significant in causing this conformational change by identifying which of those are not present with EGDMA, the only ligand which did not have a detrimental effect on BSA.

2. Materials and Methods

The crystal structure of human serum albumin (HSA) was obtained from the Protein Data Bank (PDB code 1AO6). BSA and HSA share ~90% of their primary sequence [42] which implies that they are homologous proteins with very similar crystal structures and overall biological function. HSA was employed in these studies because the crystal structure of BSA is not available in the Protein Data Bank. The ligands investigated were the same five

monomers and two crosslinkers examined in our previous work [40] – acrylamide (Aam), methacrylic acid (MAA), aminophenyl boronic acid (APBA), acrylic acid (AA), N-isopropylacrylamide (NIPAam), and N,N' methylene bisacrylamide (MBA) and ethyleneglycol dimethacrylate (EGDMA).

The docking calculations were performed using GOLD4.0. We divided the solvent accessible surface of the protein into six regions and "rolled" the ligand over these regions. Hydrogen atoms were added to the crystal structure using the TLEAP module in the AMBER10 software package. The potential energy of the protein was minimized using the AMBER99SB force field before docking. Atomic charges were assigned to the appropriate atoms in the amino acid side chains as well as those of the ligands. Genetic algorithm (GA) runs were performed for each molecule.[43] For each GA run, 2.5 million operations were applied on a set of five islands with a population size of 200. The weights for three types of operations (crossover, mutation, and migration) were chosen as 95%, 95%, and 10%, respectively. The ligands were set as flexible while the protein was rigid. The binding pockets are defined within 20 angstroms from one of six central residues selected. A total of 30 structures were generated at the end of each docking run. Although the docking was performed in vacuum, the solvent effect is implicitly modeled in the scoring function because the parameters are fit in condensed phase. Therefore, the structures are ranked with the scoring function that implicitly comprises the solvent effect.

The GOLD fitness function was used to determine the most favorable binding site for each ligand. The fitness function for GOLD is comprised of terms for protein-ligand complexation, hydrogen bonding, and internal energy of the ligand and is shown below in Equation 1.[31]

$$\begin{aligned} E_{total} &= E_{complex} + E_{H-bond} + E_{internal} \\ &= \sum_{protein}\sum_{ligand}\left(\frac{A_{ij}}{d_{ij}^{s}} - \frac{B_{ij}}{d_{ij}^{4}}\right) \\ &+ \sum_{protein}\sum_{ligand}[(E_{da}+E_{ww}) - (E_{dw}+E_{aw})] + \left\{\sum_{ligand}\left(\frac{C_{ij}}{d_{ij}^{12}} - \frac{D_{ij}}{d_{ij}^{6}}\right) + \sum_{ligand}\frac{1}{2}V\left[1+\frac{n}{|n|}cos(|n|\omega)\right]\right\} \end{aligned}$$

Equation 1

The complexation term ($E_{complex}$) is calculated from a reparameterized Lennard-Jones 8–4 potential, the hydrogen bonding term ($E_{H\text{-}bond}$) is a sum of all individual energies from the donor-acceptor pairs in the complex, and the internal energy term ($E_{internal}$) includes both a dispersion-repulsion and a torsional energy component.[26,31] In this equation, *A, B, C,* and *D* represent depth of potential well of particles a distance of *d* from each other. $E_{H\text{-}bond}$ is composed of four terms, in which *d, a, and w* represent donor, acceptor and water, respectively. A Lenard-Jones 12–6 function and Fourier series are used to describe the van der Waals and torsional interactions within the ligand ($E_{internal}$). The terms V and ω represent the force constant and the dihedral phase angle, respectively. This scoring function was originally calibrated from empirical data of 100 protein-ligand complexes.[31]

The highest scoring binding site for each ligand was specified as the pose most likely to occur when in solution with the protein experimentally. The amino acids nearest to the ligand (residues within 4Å) were identified and distances between the relevant heavy atoms of the ligand and target were measured to theorize the types of interactions occurring.

3. Results and Discussion

Docking studies provide reliable prediction of binding poses for protein-ligand interactions. As a result, we exploited this facile simulation technique to determine which amino acids surround the ligand when it is at its most favorable binding site. Also, based on the distance between the heavy atoms in the amino acid and ligand as well as the type of side group on the residue, we identified the types of interactions that are likely occurring.

3.1. Computational docking studies with common functional monomers

Clearly, when the monomer(s) are in solution with the protein at molar ratio of ligand to protein up to 2000:1 as is commonly seen in the literature, there will be far more than one ligand per protein. However, molecular docking studies give an indication as to where the ligand preferentially binds to the protein; thus, they can offer insight into the types of interactions responsible for the loss in secondary structure found in our experimental work.

Figure 1 shows the crystal structure of HSA with the seven ligands of interest located at their most favorable binding sites. HSA is a highly helical protein with 585 residues in its primary sequence and 31 α-helices present in its secondary structure.[44] Of interest is the fact that Aam, AA, NIPAam, and EGDMA preferentially bind at similar sites on the crystal structure, near residue 273 (serine). Meanwhile, MAA and APBA's favorable binding sites were near residue centers 138 (tyrosine) and 528 (alanine), respectively. This result indicates that the most favorable binding site is not based solely on ligand charge or structural similarities. If that were the case, we would expect AA and MAA to have similar binding poses. However, it also suggests that because four of the ligands bind to similar areas, they may have to compete for the same residues.

The binding pose for acrylamide (Aam) on the HSA crystal structure along with the nearby amino acids is shown in Figure 2A. Also included in this image are a few of the relevant interactions as designated by the distance between the heavy atoms of the nearby amino acids and Aam. There are six amino acids shown within the desired 4.0 Å distance – tyrosine 146, arginine 253, leucine 234, leucine 256, isoleucine 260, and alanine 287 (the numbers listed represent the actual residue in the amino acid sequence of HSA). Of those, the side groups in both tyrosine and arginine are hydrogen bonding with the ligand. Specifically, the terminal –OH on the phenol group of tyrosine is interacting with the carbonyl on Aam and two of the amine groups on the side group of arginine are within the optimal distance range for hydrogen bonding with the same functional group of Aam. The remaining four nearby residues all have hydrophobic non-polar side groups, thus are undergoing hydrophobic interactions with the ligand. In addition to this, the primary amine in Aam seems to be H-bonding with the amino group present in the polypeptide backbone at alanine (Figure 2B). This latter interaction may be the most significant of any as an explanation for the experimental circular dichroism results. This is because the hydrogen bonds along the backbone stabilize a protein's secondary structure, while the side chains are responsible for ligand binding.

Figure 3A shows methacrylic acid (MAA) in its thermodynamically favorable binding pose with five HSA residues within the specified 4 Å boundary – arginine 110, arginine 182, valine 112, arginine 113, and leucine 111. In looking closely at each of these residues, a few conclusions can be made. First, it is apparent that arginine 110 is binding both electrostatically and via H-bonding. This inference can be made based on the fact that both the positively charged amine and neutral primary amine located on the side chain of arginine are within the appropriate distance from the charged oxygen present in the carboxylate ion of MAA. The same two interactions appear to be occurring with arginine 182 and MAA. Both arginine 113 and valine 112 seem to be interacting hydrophobically via the aliphatic

groups present in their side groups and the methyl group on MAA. Lastly, MAA seems to be interacting in two ways along the polypeptide backbone at leucine 211. Specifically, the α-carbon present along the backbone is interacting hydrophobically with the vinyl group of MAA and the amino group is H-bonding with C=O group on MAA. Once again, we feel that these complexes between the ligand and the backbone are central to the protein conformational change observed experimentally.

The acrylic acid (AA) docking study reveals an analogous outcome (Figure 3B). Namely, AA appears to be interacting with seven amino acids – tyrosine 146, histidine 238, arginine 253, leucine 234, leucine 256, alanine 287, and lysine 195. The negative charge on the carboxylic acid of AA allows for electrostatic interactions with the side chains of the three positively charged residues – histidine, arginine, and lysine. Additionally, the neutral secondary amine present on arginine's side group appears to be H-bonding with the C=O group on AA. Tyrosine and the two leucine groups are interacting via H-bonding and the hydrophobic effect, respectively. Lastly, the alanine group is undergoing hydrophobic interactions with the ligand between the α-carbon along the peptide backbone and one of the carbon atoms on AA.

The same analysis was performed for aminophenylboronic acid (APBA) with HSA. In this case, eight amino acids are within the desired distance – glutamine 576, glutamic acid 497, lysine 532, alanine 578, serine 575, histidine 531, phenylalanine 498, and lysine 528 (Figure 3C). The histidine, phenylalanine, and leucine residues are all undergoing hydrophobic interactions between carbons on the side chains and carbon atoms in the phenyl ring of APBA. Not surprisingly, APBA is the only ligand of the seven which its binding pose is near a phenylalanine residue.

The remaining five residues listed above appear to be hydrogen bonding to APBA. Furthermore, three of these – glutamic acid, alanine, and serine – exhibit H-bonding between their C=O groups along the peptide backbone and the primary amine of APBA (or the boronic acid group in the case of glutamic acid). Additionally, since APBA is positively charged and glutamic acid is negatively charged at neutral pH conditions, these two are interacting electrostatically. The finding that three interactions are occurring between the peptide backbone and APBA can help explain the precipitous drop in helical structure for BSA which occurs at a ligand concentration much lower than that of the other monomers.[40]

Figure 3D shows the favorable binding pose for the amphiphilic monomer, N-isopropylacrylamide (NIPAam). Crosslinked P(NIPAam) is commonly studied for biomedical applications as a temperature responsive polymer due to its reversible swelling properties near physiological temperatures.[45] This behavior is a result of the competition between strong hydrophobic interactions and hydrogen bonding that is temperature dependent. In our analysis here, we found ten amino acids responsible for these two types of interactions – arginine 253, tyrosine 146, lysine 146, leucine 234, valine 237, histidine 238, leucine 256, alanine 257, isoleucine 260, and alanine 287. Hydrophobic interactions are occurring between the hydrophobic isopropyl group on NIPAam and the side chains of lysine, valine, histidine, isoleucine, alanine 287, as well as both leucine residues. Arginine and tyrosine are undergoing hydrogen bonding with the carbonyl group on the ligand. Lastly, NIPAam is interacting hydrophobically with the backbone α-carbon of alanine 257.

It is interesting to note that hydrogen bonding and hydrophobic interactions play such a large role in these complexes even with charged ligands. In looking overall at all of the interactions occurring for these five monomers it seems that hydrophobic interactions are the most important of the three, followed by H-bonding – based on quantity alone. Obviously, this statement does not take into account the relative strength of each of these interactions,

which molecular docking does not provide. However, it is clear that both hydrogen bonding and hydrophobic interactions have a significant role in the ligand binding and conformational change of the protein.

In general, it is apparent that in addition to the interactions occurring between the amino acid side chains and the ligands investigated, there is also at least one interaction taking place for each of the ligands with the polypeptide backbone. Arginine and alanine are the residues which seem to be interacting the most frequently with the ligands as these two are nearby four of the five monomers. On the other hand, there are several amino acids not near any of the ligands – aspartic acid, proline, glycine, methionine, tryptophan, threonine, cysteine, and asparagine. Further studies with larger sets of monomers are required before we can make sweeping statements about the lack of importance of these amino acids in monomer-template complexation.

In looking at the four ligands with a similar binding site near residue 273 (Aam, AA, and NIPAam), they seem to share several common amino acids. Specifically, tyrosine 146, arginine 253, leucine 234, and leucine 256 are all interacting with these four ligands. This result sheds light into the complexity of a pre-polymerization solution in which multiple monomers are included as these ligands compete for the same amino acids. This competition can also help explain the limited success in the field to date as two or three monomers are often employed in the synthesis of protein MIPs.

3.2. Computational docking studies with common crosslinkers

Next, similar analyses were performed for the two most common crosslinkers, N, N' methelenebisacrylamide (MBA) and ethyleneglycol dimethacrylate (EGDMA). Figure 3E shows the favorable binding pose for MBA with HSA. Eight amino acids are undergoing non-covalent interactions with the ligand – serine 61, glutamic acid 91, histidine 243, leucine 62, histidine 63, proline 92, and asparagine 95. Hydrophobic interactions are taking place between the carbons on MBA and carbon atoms on the side chain of serine, proline, asparagine, and both histidine residues. Side chain hydrogen bonding is occurring with glutaminc acid and serine with the ligand. Once again, interactions do seem to be occurring between MBA and the backbone of leucine 62. In this particular case, both hydrogen bonding (between amino group and C=O on MBA) and hydrophobic interactions (between α-carbon of backbone and the vinyl group on MBA) are taking place.

The docking studies with EGDMA are important as this was the only ligand which did not induce a significant protein conformational change in the circular dichroism studies. Identifying a difference in the type of interactions occurring with EGDMA relative to the other six ligands would allow for a rational explanation of why the protein was not susceptible to EGDMA. Using the same analysis, six amino acids are potentially interacting with EGDMA – arginine 218, arginine 253, tyrosine 146, lysine 191, lysine 195, and leucine 256 (Figure 4A). Side chain hydrogen bonding appears to be happening between the C=O groups on EGDMA and the terminal amines present in the two arginine residues as well as with the alcohol group on tyrosine. Additionally, the carbons on the side chains of the two lysine and leucine residues are undergoing hydrophobic interactions with various carbon atoms present on EGDMA. EGDMA's binding site is near residue 273 and we see, once again, that tyrosine 146, arginine 253, and leucine 256 are near the ligand. These are the same amino acids that neighbor the other three ligands whose binding poses are in the same vicinity (Aam, AA, and NIPAam).

Of note here is the fact that there are no interactions seem to be occurring with atoms present along the backbone of any neighboring residues. In our previous work,[40,46] we postulate that the reason for the lack of detrimental effects on the protein' structure was due to the absence

of hydrogen-bonding donors present in EGDMA's structure. Indeed, there is a potential H-bonding location along the backbone of a nearby alanine (between carbonyl group in alanine's backbone and carbonyl group of EGDMA); however, since EGDMA does not have hydrogen donor, no such interaction can occur (Figure 4B). Since EGDMA is interacting both hydrophobically and via H-bonding with the side chain of various amino acids, the only major difference between the results of docking analysis of EGDMA and the other six ligands is the absence of a backbone interaction. As a result, we conclude that it is the disruption of non-covalent interactions (H-bonding, electrostatic, and/or hydrophobic) along the polypeptide backbone which results in the loss of conformation when the protein is in solution with these ligands.

4. Conclusions

The molecular docking studies of HSA with common monomers and crosslinkers from protein MIPs show that significant amounts of hydrogen bonding as well as electrostatic and hydrophobic interactions are occurring between the target and ligand. Our original hypothesis of disruption in hydrogen bonds was confirmed to a certain extent. It appears that the other two main types of non-covalent interactions also contribute to this phenomenon, but only if they are taking place with atoms along the polypeptide backbone. This is a reasonable conclusion because the interactions which define the secondary structure take place between atoms along the backbone while those with the side chains are indicative of ligand binding. We postulate that the interactions with the side chain functional groups seen in these docking studies account for a portion of the CD spectra change observed experimentally.[40] Specifically, the lowest few concentrations of ligand resulted in only a change in molar ellipticity without loss in characteristic shape for albumin's CD spectra (i.e. minimal drop in α-helical %). However, once the concentration of ligand is increased, the interactions with the peptide backbone begin to dominate causing significant disruption in the helical structures present in the protein.

Additionally, we identified several specific amino acids which the various ligands are interacting. This finding offers another explanation as to why success has been limited to date. Namely, if monomers are preferentially binding to the same amino acids, then the use of multiple monomers in the pre-polymerization solution, which is often done in the literature, can give rise to non-specific interactions as a result of this competition.

Acknowledgments

The authors acknowledge financial support from the National Science Foundation (D.K. is a NSF Graduate Research Fellow) and the National Institutes of Health for grant support to P.R. (R01GM079686).

References

1. Bergmann N, Peppas NA. Molecularly imprinted polymers with specific recognition for macromolecules and proteins. Progress in Polymer Science. 2008; 33:271–288.
2. Bures P, Huang YB, Oral E, Peppas NA. Surface modifications and molecular imprinting of polymers in medical and pharmaceutical applications. Journal of Controlled Release. 2001; 72(1–3): 25–33. [PubMed: 11389982]
3. Hilt JZ, Byrne ME. Configurational biomimesis in drug delivery: molecular imprinting of biologically significant molecules. Adv. Drug Deliv. Rev. 2004; 56(11):1599–1620. [PubMed: 15350291]
4. Kryscio DR, Peppas NA. Mimicking Biological Delivery Through Feedback-Controlled Drug Release Systems Based on Molecular Imprinting. AIChE Journal. 2009; 55(6):1311–1324.
5. Oral E, Peppas NA. Molecular imprinting in biological systems. Stp Pharma Sciences. 2000; 10(4): 261–267.

6. Turner NW, Jeans CW, Brain KR, Allender CJ, Hlady V, Britt DW. From 3D to 2D: A Review of the Molecular Imprinting of Proteins. Biotechnology Progress. 2006; 22:1474–1489. [PubMed: 17137293]
7. Chianella I, Lotierzo M, Piletsky SA, Tothill IE, Chen BN, Karim K, Turner APF. Rational design of a polymer specific for microcystin-LR using a computational approach. Analytical Chemistry. 2002; 74(6):1288–1293. [PubMed: 11924591]
8. Henthorn DB, Peppas NA. Molecular simulations of recognitive behavior of molecularly imprinted intelligent polymeric networks. Industrial & Engineering Chemistry Research. 2007; 46(19):6084–6091.
9. Karlsson BCG, O'Mahony J, Karlsson JG, Bengtsson H, Eriksson LA, Nicholls IA. Structure and Dynamics of Monomer-Template Complexation: An Explanation for Molecularly Imprinted Polymer Recognition Site Heterogeneity. Journal of the American Chemical Society. 2009; 131(37):13297–13304. [PubMed: 19708659]
10. Nicholls IA, Andersson HS, Charlton C, Henschel H, Karlsson BCG, Karlsson JG, O'Mahony J, Rosengren AM, Rosengren KJ, Wikman S. Theoretical and computational strategies for rational molecularly imprinted polymer design. Biosensors and Bioelectronics. 2009; 25(3):543–552. [PubMed: 19443204]
11. Pavel D, Lagowski J. Computationally designed monomers and polymers for molecular imprinting of theophylline and its derivatives. Part I. Polymer. 2005; 46(18):7528–7542.
12. Piletsky SA, Karim K, Piletska EV, Day CJ, Freebairn KW, Legge C, Turner APF. Recognition of ephedrine enantiomers by molecularly imprinted polymers designed using a computational approach. Analyst. 2001; 126(10):1826–1830.
13. Hsu CY, Lin HY, Thomas JL, Wu BT, Chou TC. Incorporation of styrene enhances recognition of ribonuclease A by molecularly imprinted polymers. Biosensors and Bioelectronics. 2006; 22(3): 355–363. [PubMed: 16781138]
14. Levi L, Srebnik S. Simulation of Protein-Imprinted Polymers. 1. Imprinted Pore Properties. Journal of Physical Chemistry B. 2010; 114(1):107–114.
15. Levi L, Srebnik S. Simulation of Protein-Imprinted Polymers. 2. Imprinting Efficiency. Journal of Physical Chemistry B. 2010; 114(50):16744–16751.
16. Pan J, Xue XH, Wang JH, Me HM, Wu ZY. Recognition property and preparation of Staphylococcus aureus protein A-imprinted polyacrylamide polymers by inverse-phase suspension and bulk polymerization. Polymer. 2009; 50(11):2365–2372.
17. Bergmann NM, Peppas NA. Configurational Biomimetic Imprinting for Protein Recognition: Structural Characteristics of Recognitive Hydrogels. Industrial & Engineering Chemistry Research. 2008; 47(23):9099–9107.
18. Janiak DS, Ayyub OB, Kofinas P. Effects of Charge Density on the Recognition Properties of Molecularly Imprinted Polymeric Hydrogels. Macromolecules. 2009; 42(5):1703–1709.
19. Doman TN, McGovern SL, Witherbee BJ, Kasten TP, Kurumbail R, Stallings WC, Connolly DT, Shoichet BK. Molecular docking and high-throughput screening for novel inhibitors of protein tyrosine phosphatase-1B. Journal of Medicinal Chemistry. 2002; 45(11):2213–2221. [PubMed: 12014959]
20. Paiva AM, Vanderwall DE, Blanchard JS, Kozarich JW, Williamson JM, Kelly TM. Inhibitors of dihydrodipicolinate reductase, a key enzyme of the diaminopimelate pathway of Mycobacterium tuberculosis. Biochimica Et Biophysica Acta-Protein Structure and Molecular Enzymology. 2001; 1545(1–2):67–77.
21. Pearlman DA, Case DA, Caldwell JW, Ross WS, Cheatham TE, Debolt S, Ferguson D, Seibel G, Kollman P. Amber, a Package of Computer-Programs for Applying Molecular Mechanics, Normal-Mode Analysis, Molecular-Dynamics and Free-Energy Calculations to Simulate the Structural and Energetic Properties of Molecules. Computer Physics Communications. 1995; 91(1–3):1–41.
22. Jorgensen WL, Maxwell DS, TiradoRives J. Development and testing of the OPLS all-atom force field on conformational energetics and properties of organic liquids. Journal of the American Chemical Society. 1996; 118(45):11225–11236.

23. MacKerell AD. Developments in the CHARMM all-atom empirical energy function for biological molecules. Abstracts of Papers of the American Chemical Society. 1998; 216:U696–U696.
24. Essex JW, Taylor RD, Jewsbury PJ. A review of protein-small molecule docking methods. Journal of Computer-Aided Molecular Design. 2002; 16(3):151–166. [PubMed: 12363215]
25. Ewing TJA, Makino S, Skillman AG, Kuntz ID. DOCK 4.0: Search strategies for automated molecular docking of flexible molecule databases. Journal of Computer-Aided Molecular Design. 2001; 15(5):411–428. [PubMed: 11394736]
26. Jones G, Willett P, Glen RC, Leach AR, Taylor R. Development and validation of a genetic algorithm for flexible docking. Journal of Molecular Biology. 1997; 267(3):727–748. [PubMed: 9126849]
27. Rarey M, Kramer B, Lengauer T, Klebe G. A fast flexible docking method using an incremental construction algorithm. Journal of Molecular Biology. 1996; 261(3):470–489. [PubMed: 8780787]
28. Friesner RA, Murphy RB, Repasky MP, Frye LL, Greenwood JR, Halgren TA, Sanschagrin PC, Mainz DT. Extra precision glide: Docking and scoring incorporating a model of hydrophobic enclosure for protein-ligand complexes. Journal of Medicinal Chemistry. 2006; 49(21):6177–6196. [PubMed: 17034125]
29. Jorgensen WL. The many roles of computation in drug discovery. Science. 2004; 303(5665):1813–1818. [PubMed: 15031495]
30. Plewczynski D, Lazniewski M, Augustyniak R, Ginalski K. Can We Trust Docking Results? Evaluation of Seven Commonly Used Programs on PDBbind Database. J. Comput. Chem. 2011; 32(4):742–755. [PubMed: 20812323]
31. Wang RX, Lu YP, Wang SM. Comparative evaluation of 11 scoring functions for molecular docking. Journal of Medicinal Chemistry. 2003; 46(12):2287–2303. [PubMed: 12773034]
32. Ramos MJ, Sousa SF, Fernandes PA. Protein-ligand docking: Current status and future challenges. Proteins-Structure Function and Bioinformatics. 2006; 65(1):15–26.
33. Yang TY, Wu JC, Yan CL, Wang YF, Luo R, Gonzales MB, Dalby KN, Ren PY. Virtual screening using molecular simulations. Proteins-Structure Function and Bioinformatics. 2011; 79(6):1940–1951.
34. Anfinsen CB. Principles that govern the folding of protein chains. Science. 1973; 181(4096):223–230. [PubMed: 4124164]
35. Kauzmann W. Some factors in the interpretation of protein denaturation. Advances in Protein Chemistry. 1959; 14:1–63. [PubMed: 14404936]
36. Branden, C.; Tooze, J. Introduction to protein structure. New York: Garland Publishing; 1999. Folding and Flexibility.
37. Manning MC, Chou DK, Murphy BM, Payne RW, Katayama DS. Stability of Protein Pharmaceuticals: An Update. Pharmaceutical Research. 2010; 27(4):544–575. [PubMed: 20143256]
38. Lim WK, Rosgen J, Englander SW. Urea, but not guanidinium, destabilizes proteins by forming hydrogen bonds to the peptide group. Proceedings of the National Academy of Sciences of the United States of America. 2009; 106(8):2595–2600. [PubMed: 19196963]
39. Canchi DR, Paschek D, Garcia AE. Equilibrium Study of Protein Denaturation by Urea. Journal of the American Chemical Society. 2010; 132(7):2338–2344. [PubMed: 20121105]
40. Kryscio DR, Fleming MQ, Peppas NA. Protein conformational studies for molecularly imprinted polymers. J Molec Recogn. submitted.
41. Halperin I, Ma BY, Wolfson H, Nussinov R. Principles of docking: An overview of search algorithms and a guide to scoring functions. Proteins-Structure Function and Genetics. 2002; 47(4):409–443.
42. Peters, T. All About Albumin: Biochemistry, Genetics, and Medical Applications. San Diego, CA: Academic Press; 1996.
43. Olson AJ, Morris GM, Goodsell DS, Halliday RS, Huey R, Hart WE, Belew RK. Automated docking using a Lamarckian genetic algorithm and an empirical binding free energy function. Journal of Computational Chemistry. 1998; 19(14):1639–1662.

44. Matsuo K, Yonehara R, Gekko K. Secondary-structure analysis of proteins by vacuum-ultraviolet circular dichroism spectroscopy. Journal of Biochemistry. 2004; 135(3):405–411. [PubMed: 15113839]

45. Qiu Y, Park K. Environment-sensitive hydrogels for drug delivery. Adv. Drug Deliv. Rev. 2001; 53(3):321–339. [PubMed: 11744175]

46. Kryscio DR, Fleming MQ, Peppas NA. Conformational studies of common templates for macromolecularly imprinted polymers. Biosensors and Bioelectronics. submitted.

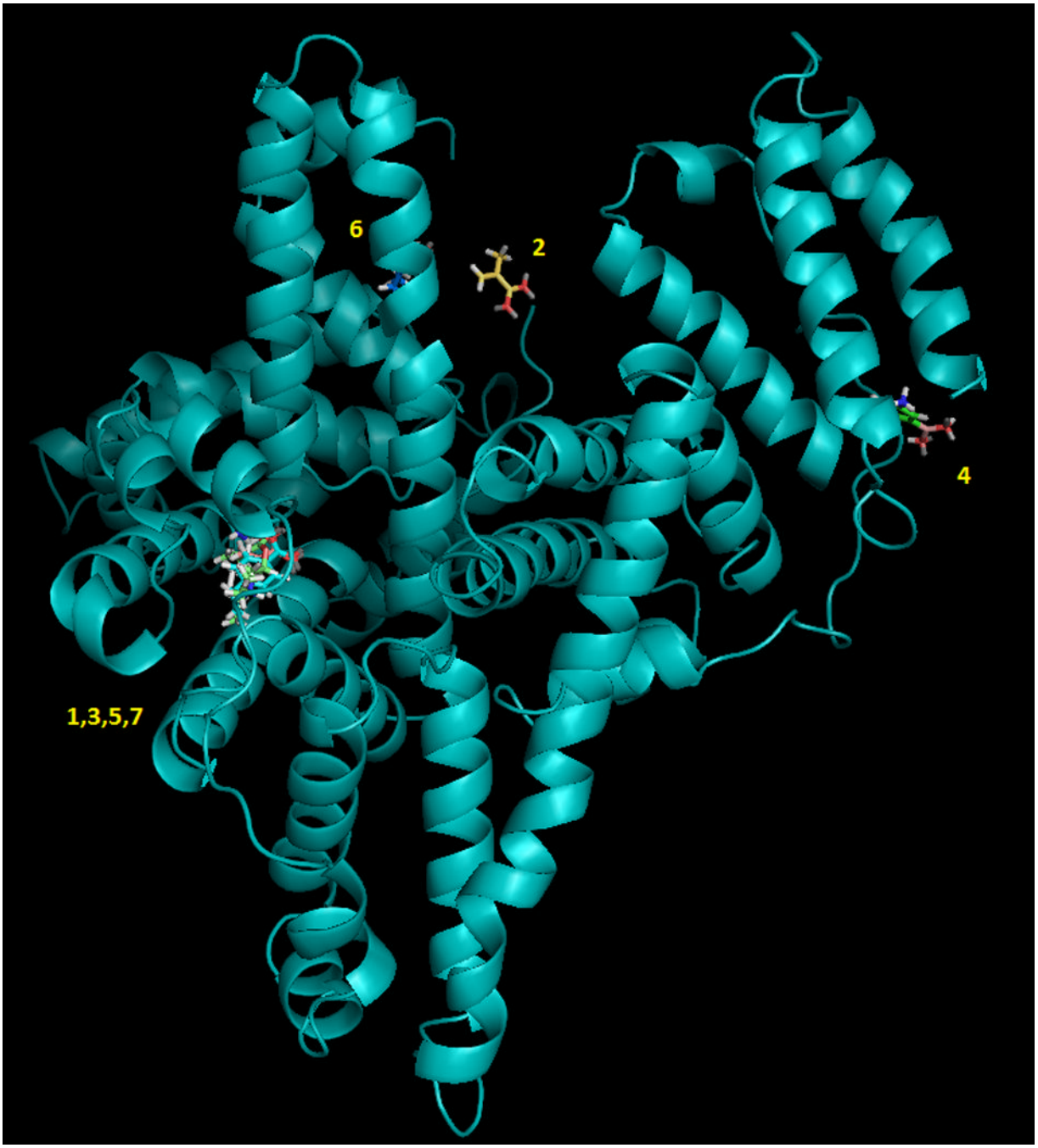

Figure 1.
Docking studies showing best binding site for all seven ligands investigated to the HSA crystal structure. Favorable binding pose for (1) acrylamide (Aam), (2) methacrylic acid (MAA), (3) acrylic acid (AA), (4) aminophenylboronic acid (APBA), (5) N-isopropylacrylamide (NIPAam), (6) methylenebisacrylamide (MBA), and (7) ethyleneglycol dimethacrylate (EGDMA).

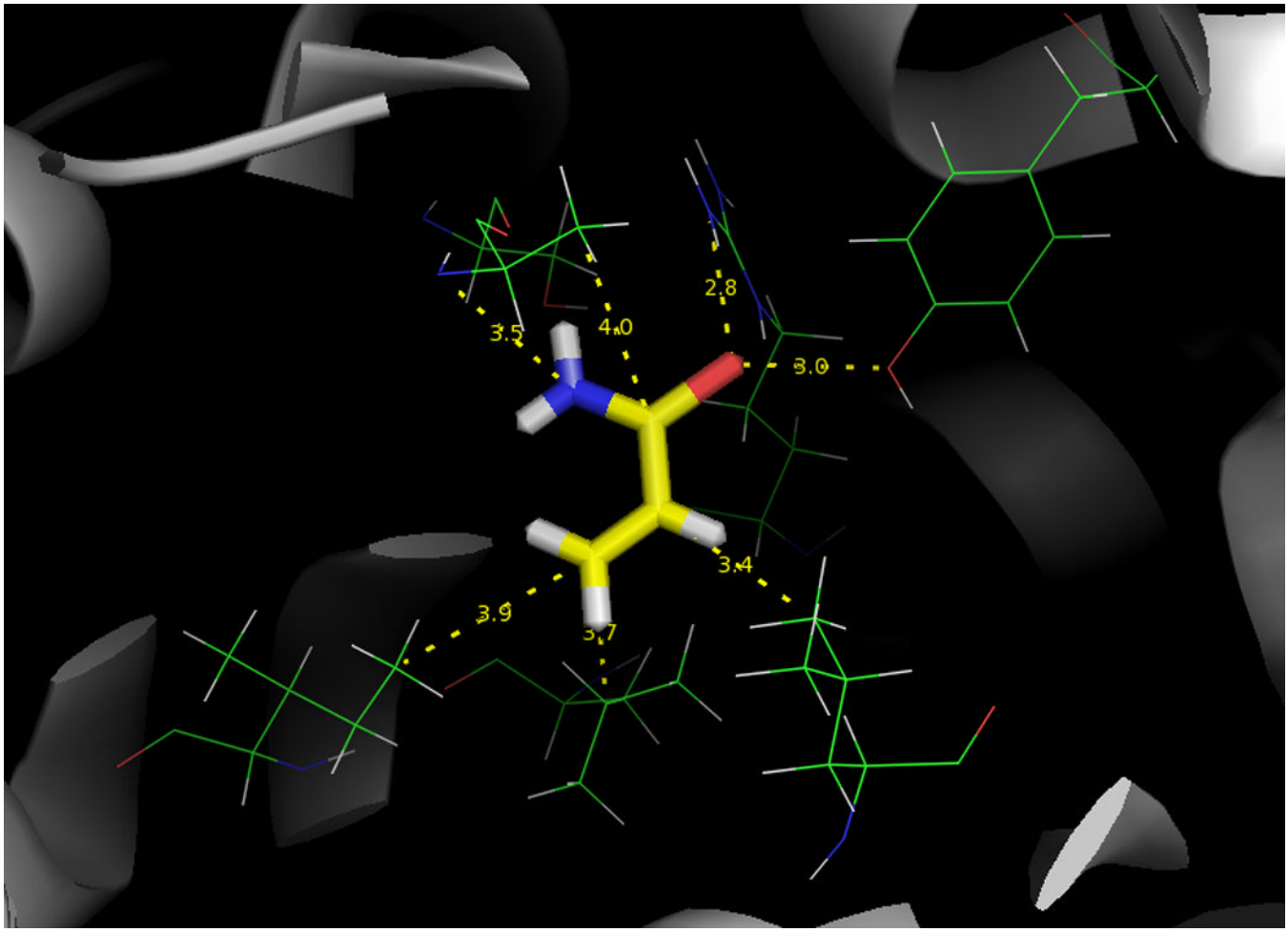

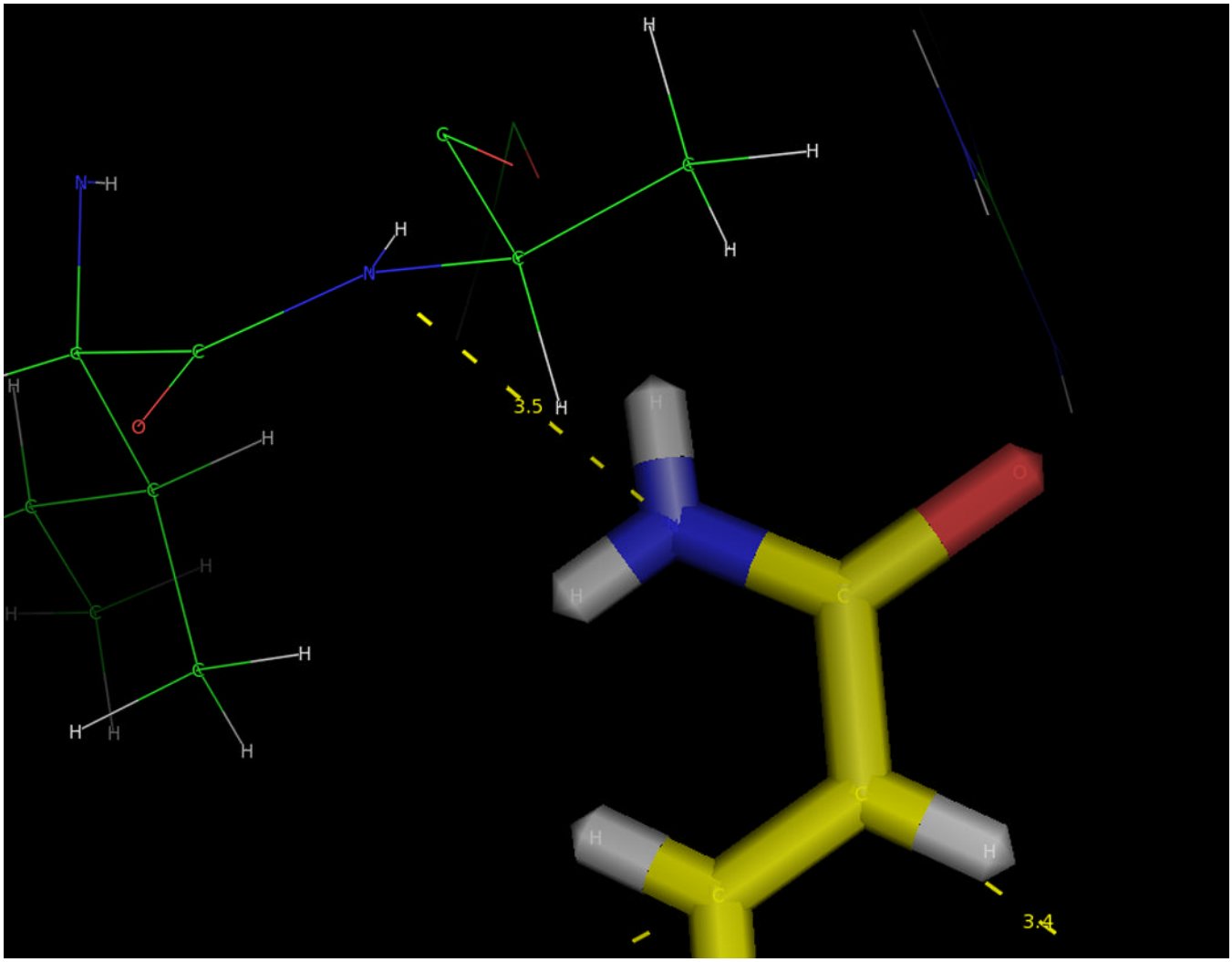

Figure 2.
(A) HSA amino acids surrounding acrylamide (Aam) when at its most favorable binding site. Also included are a few representative distances between relevant heavy atoms of the ligand and amino acid residues. (B) Hydrogen boding occurring between amide group on Aam and amine group present in polypeptide backbone at alanine 287. Distances given in Å. Carbon atoms are yellow (ligand) or green (amino acid), oxygen atoms are red, nitrogen atoms are blue, hydrogen atoms are white, and lone pairs are gray.

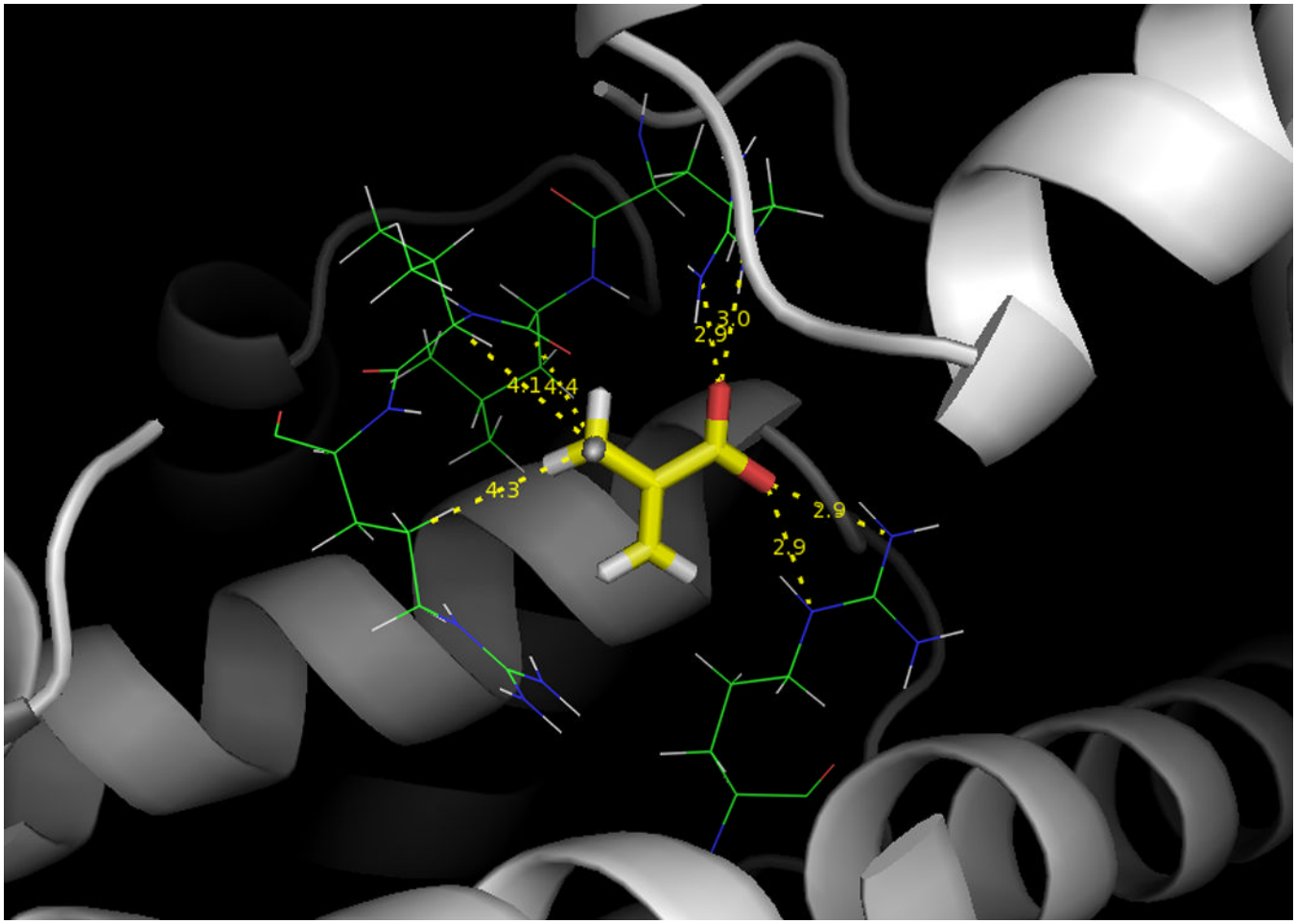

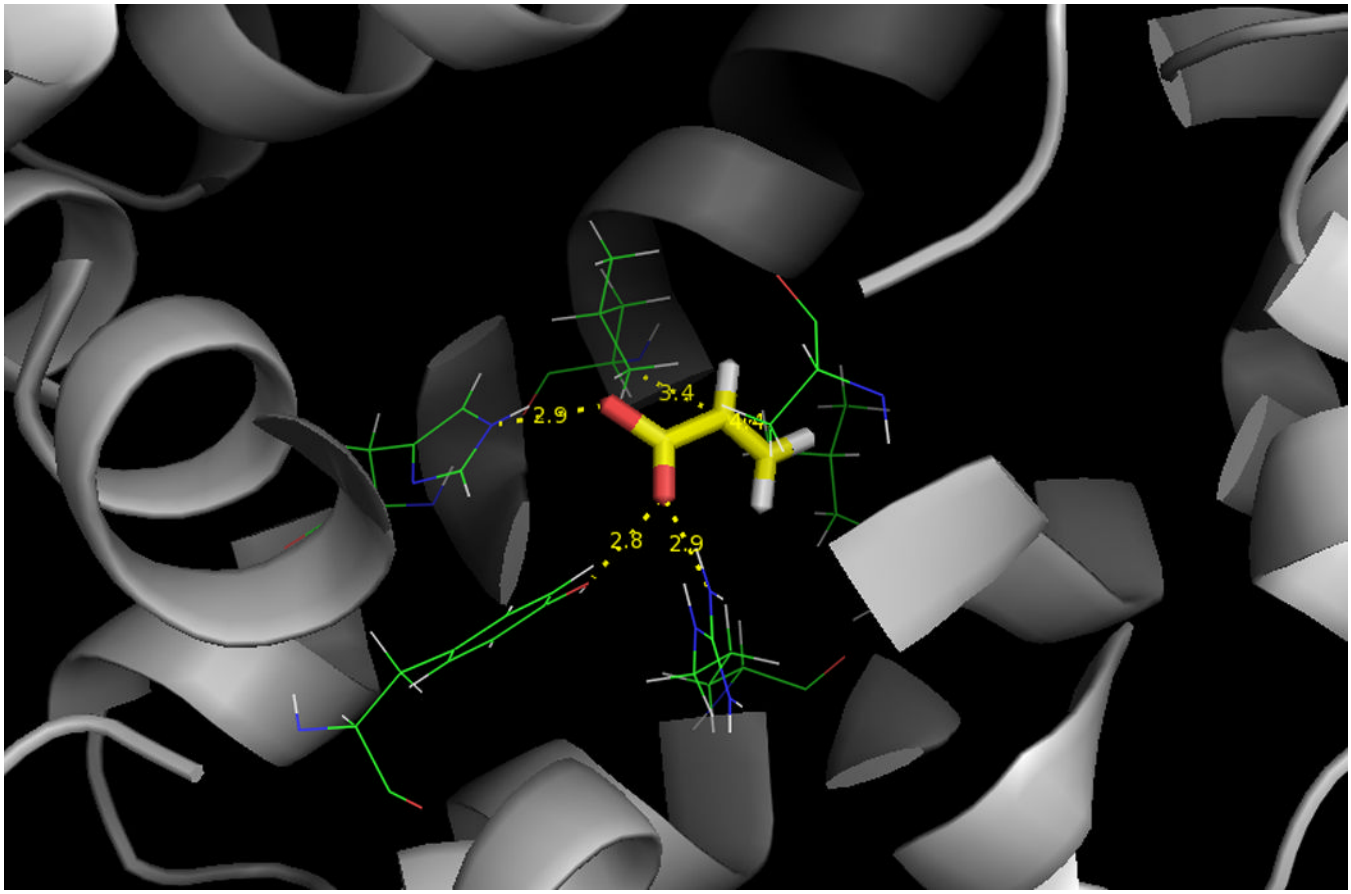

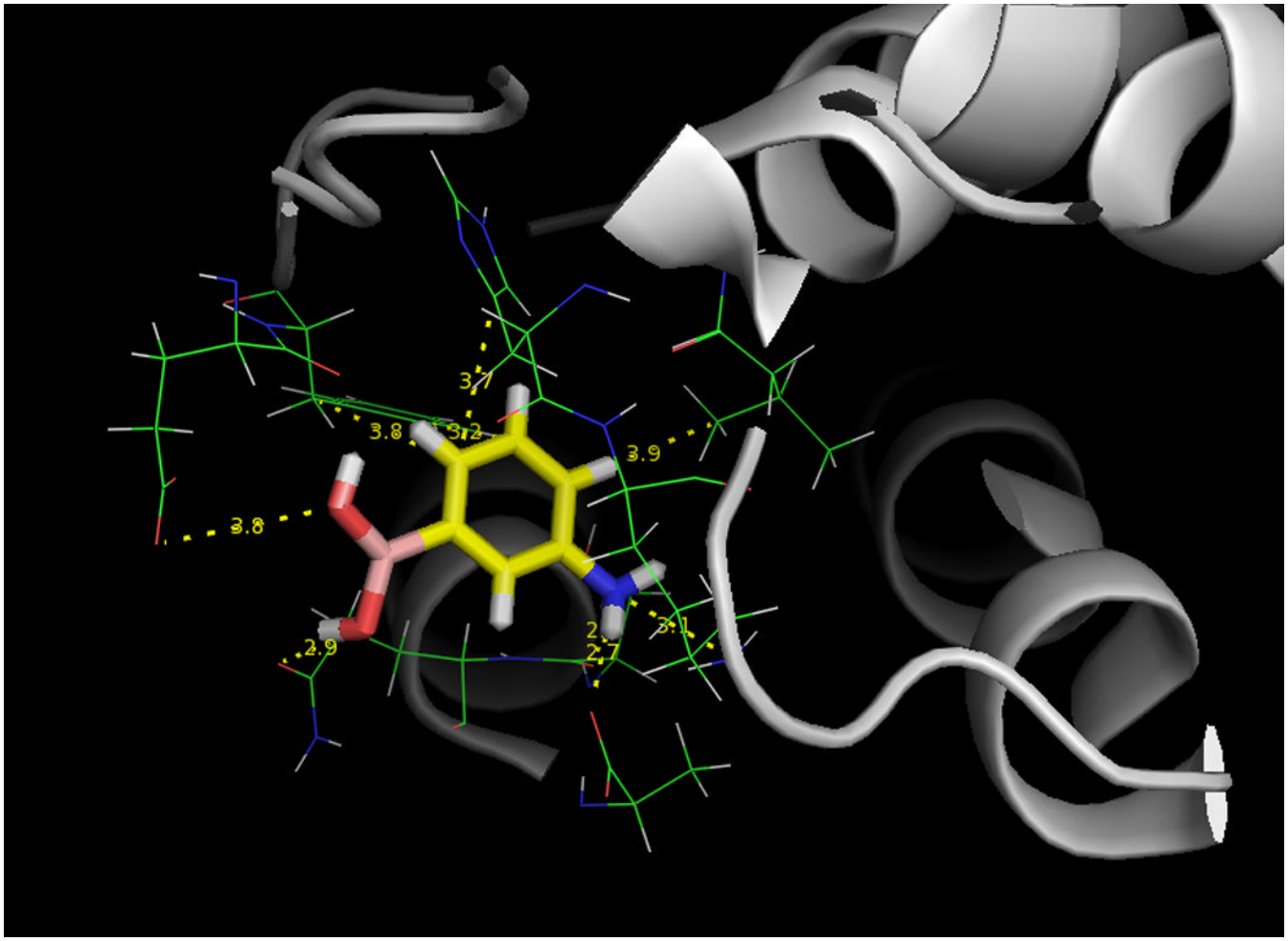

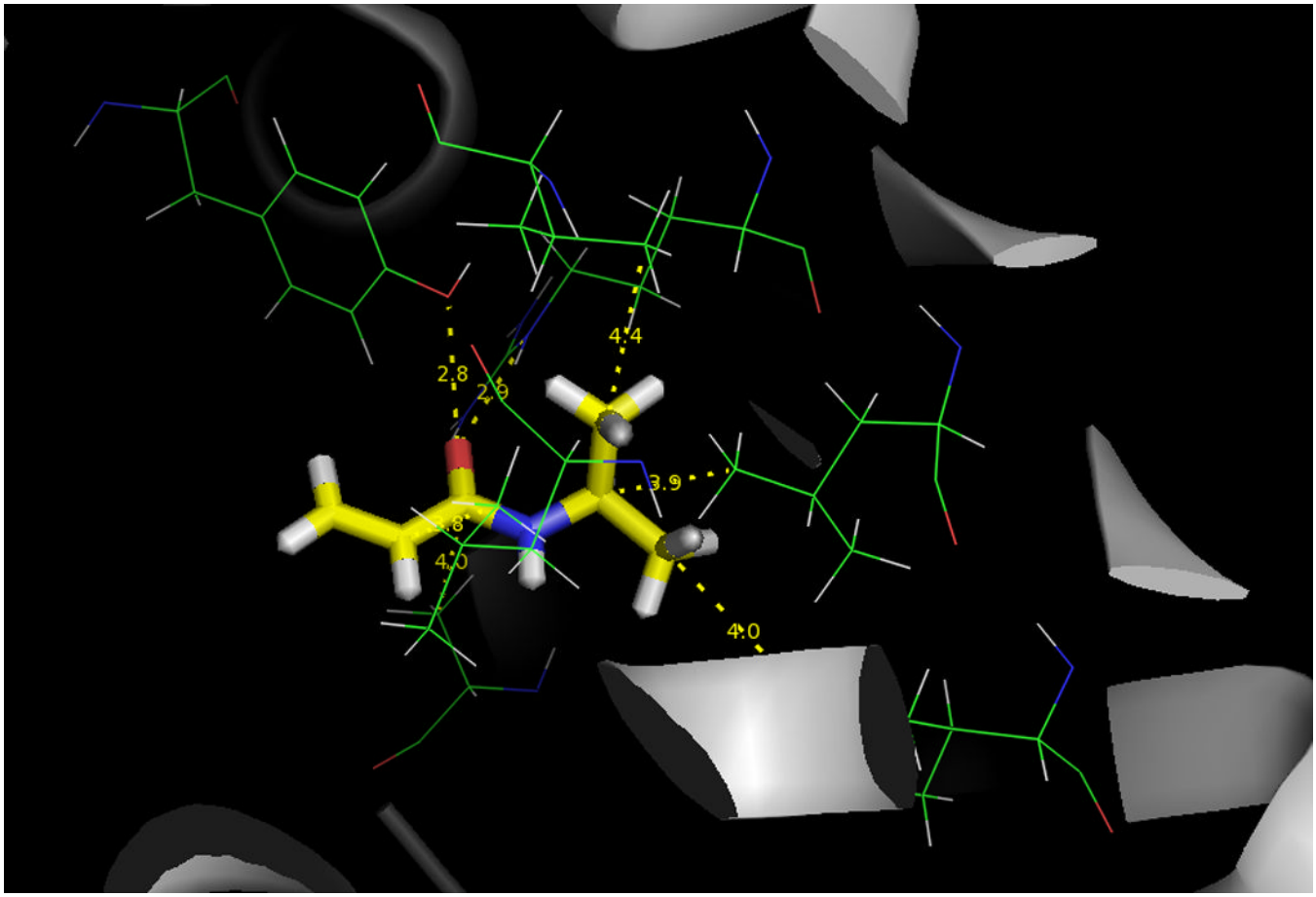

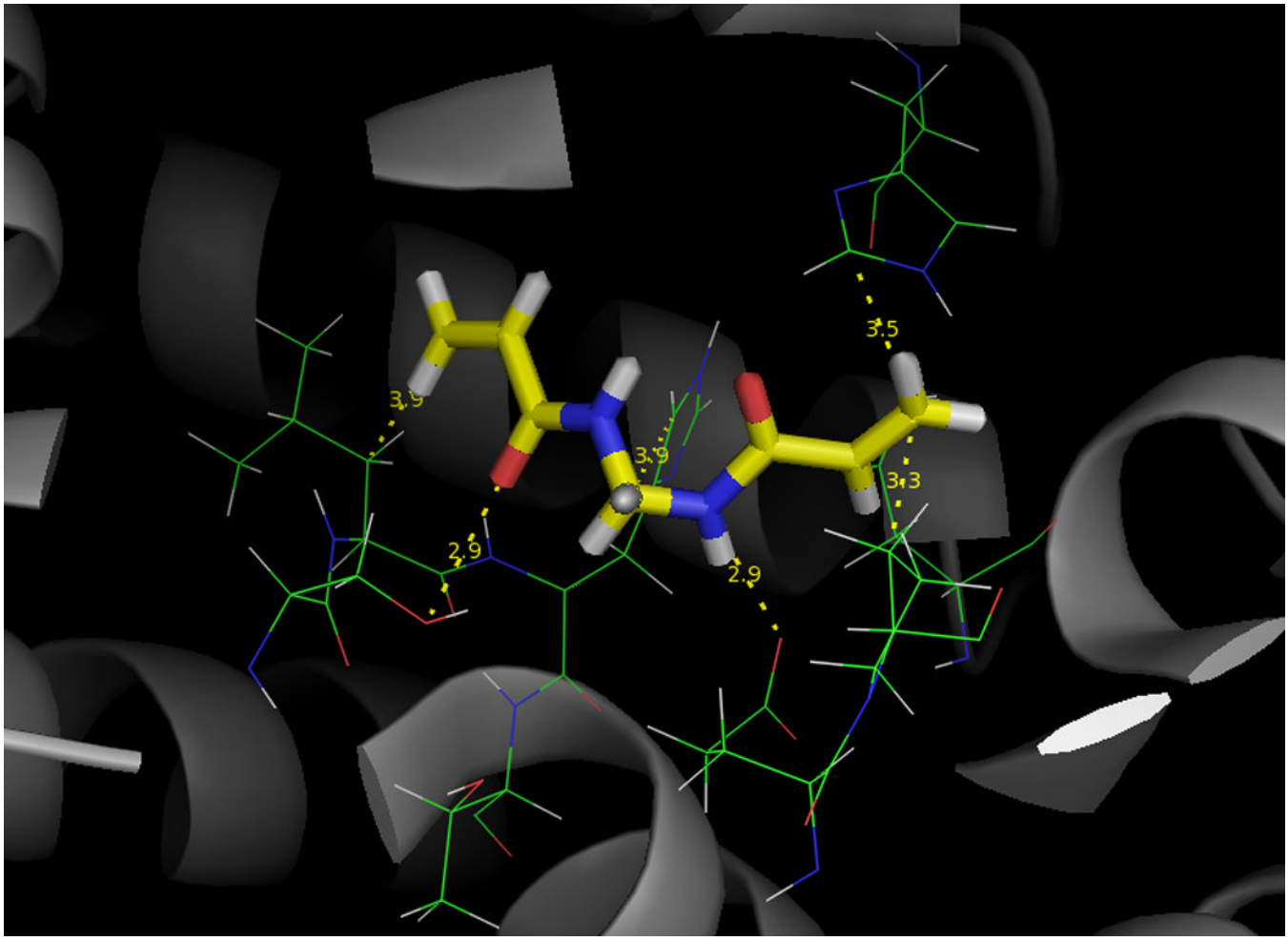

Figure 3.

HSA amino acids surrounding (A) methacrylic acid (MAA); (B) acrylic acid (AA); (C) 3-aminophenylboronic acid (APBA); (D) N-isopropyl acrylamide (NIPAam); and (E) N,N' methylenebisacrylamide (MBA) when at their most favorable binding sites. Included are a few representative distances between relevant heavy atoms of the ligand and amino acid residues for each protein-ligand pair. Distances given in Å. Carbon atoms are yellow (ligand) or green (amino acid), oxygen atoms are red, nitrogen atoms are blue, hydrogen atoms are white, and boron atoms are pink.

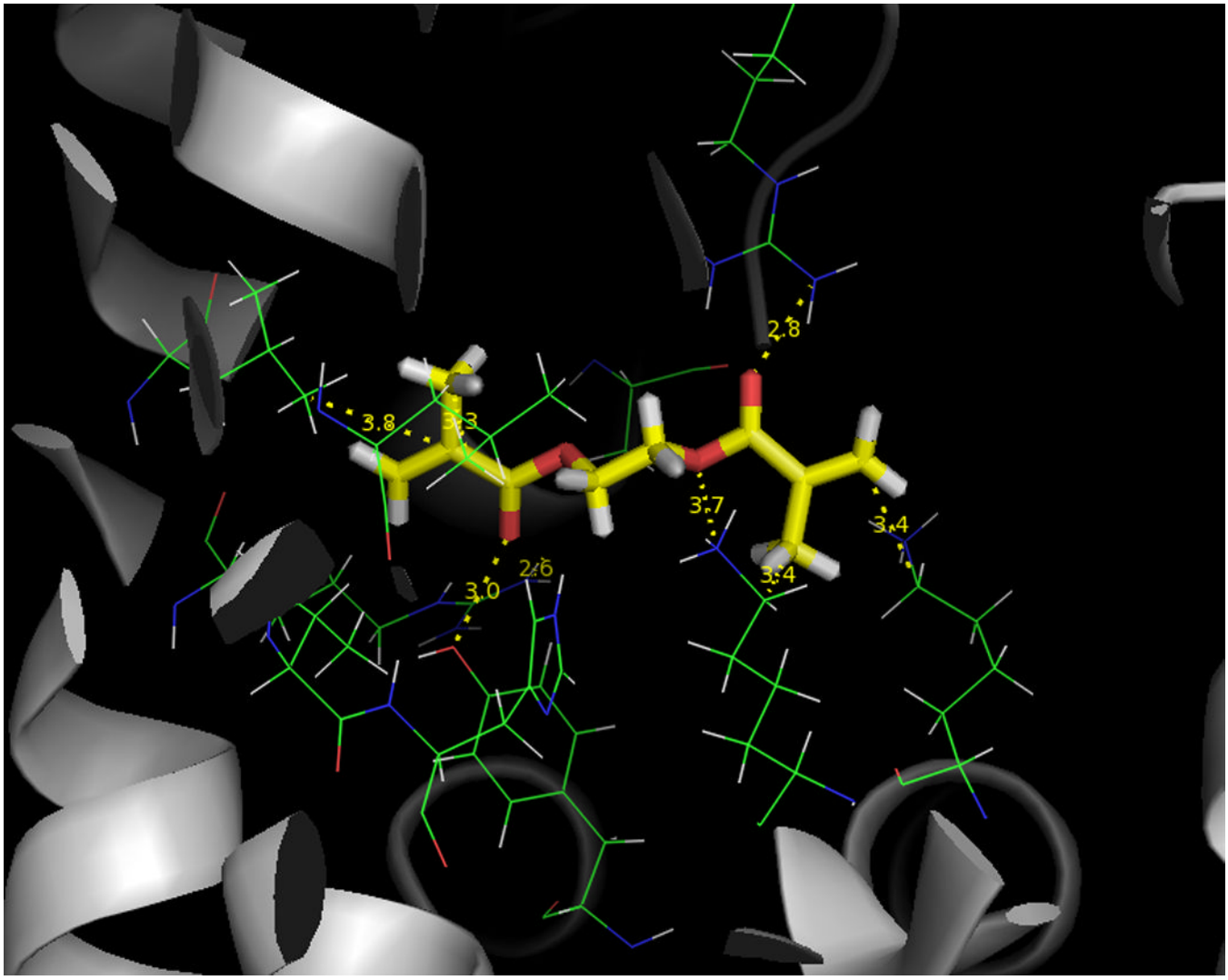

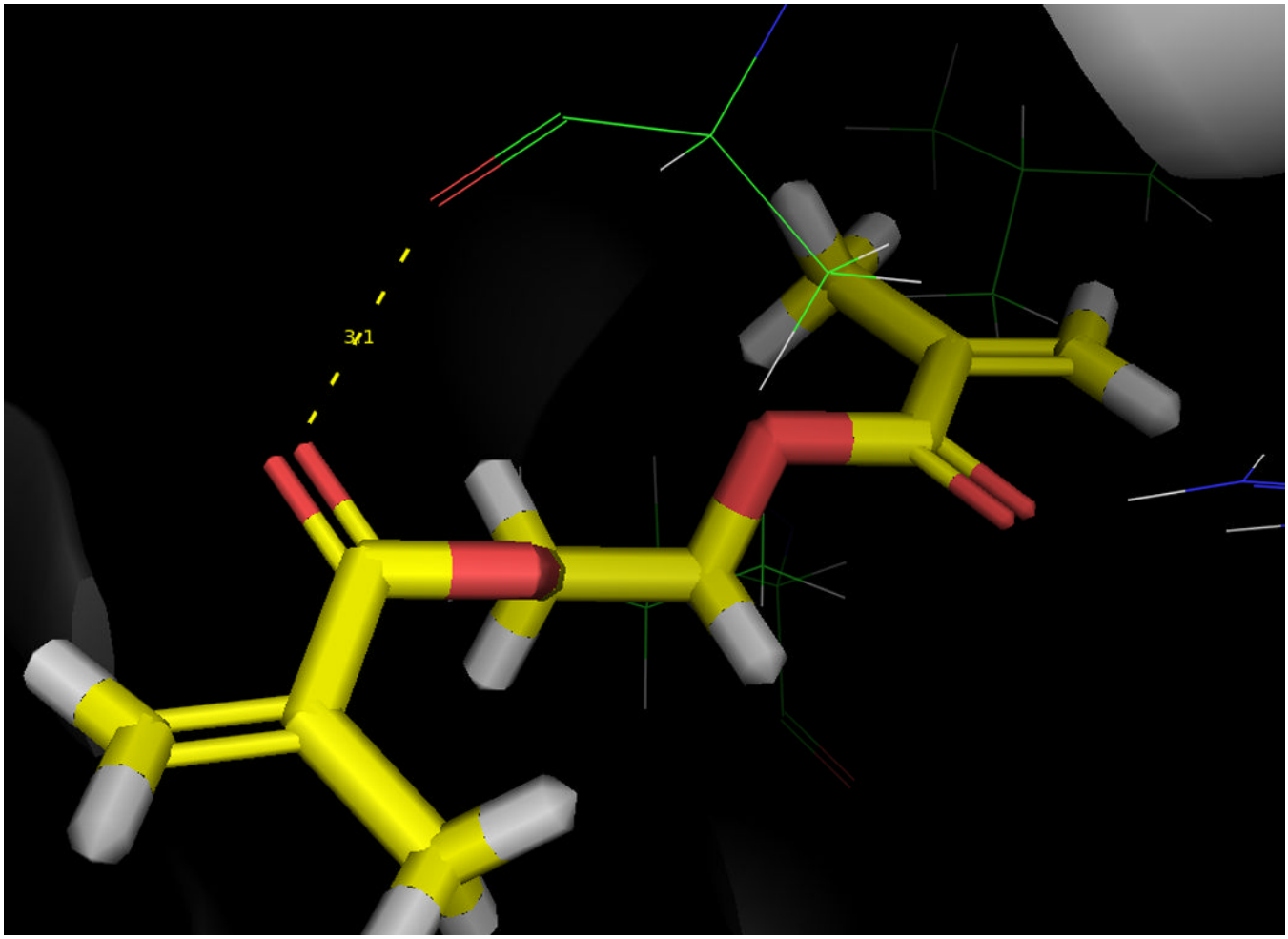

Figure 4.
(A) HSA amino acids surrounding ethyleneglycol dimethacrylate (EGDMA) when at its most favorable binding site. Only interactions with pendant amino acid groups are taking place. (B) Absence of a Hydrogen bond donor on EGDMA's structure prevents possible interaction from taking place with carbonyl group in polypeptide backbone at alanine 287. Distances given in Å. Carbon atoms are yellow (ligand) or green (amino acid), oxygen atoms are red, nitrogen atoms are blue, and hydrogen atoms are white.